Materials Science Forum
ISSN: 1662-9752, Vol. 925, pp 257-263
doi:10.4028/www.scientific.net/MSF.925.257

Submitted: 2017-07-05
Revised: 2017-12-15
Accepted: 2018-01-10
Online: 2018-06-20

Correlation between Solidification Time and Cooling Rate, Microstructure and Tensile Strength of a Low Alloyed Grey Cast Iron

Pål Schmidt

Volvo Powertrain Corp. Dept. BF67320, VLU2, S-405 08 Gothenburg, Sweden

pal.schmidt@volvo.com

Keywords: grey cast iron, microstructure, solidification time, cooling rate, tensile strength

Background. Despite more than hundred years of research the quantitative relation between microstructure and tensile strength of pearlitic grey irons is not fully understood. Ever since the classic paper of Schneidewind and McElwee in 1950 [1] a large number of relations based on regression analysis of chemical composition and wall thickness have been developed. However, microstructural features like fraction of primary austenite, size and shape of the graphite as well as pearlite fineness are seldom included in these equations. More recently, a number of examples of the latter type have appeared.

It is a well-known fact that tensile strength of grey cast irons is inversely proportional to the (square root of) graphite flake size, see Fig. 1.

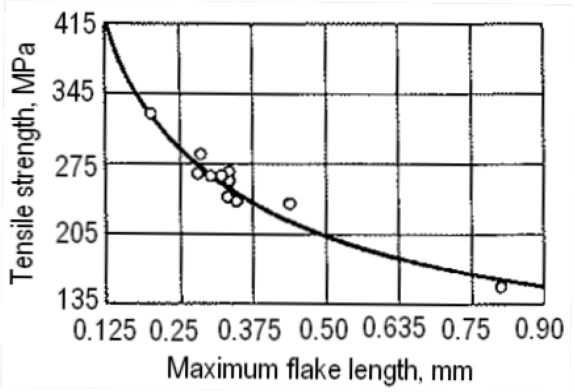

Figure 1. UTS vs. maximum graphite flake length [2].

Catalina et al. [3] developed an equation where maximum graphite flake length and pearlite lamellar spacing are the two parameters, see Eq. 1.

$$\sigma = k_1 + \frac{k_3}{\sqrt{L_{max}}} + \frac{k_4}{\sqrt{L_{max} \times \lambda_p}} \quad (1)$$

Mampaey [4] made experiments where he managed to separate the influence of solidification time and eutectoid cooling rate by placing his samples in a furnace right after solidification. He found that faster cooling rate through the eutectoid range can increase tensile strength up to 50 MPa by refinement of the pearlite.

Fourlakidis et al [5] adopted an entirely new approach by introducing the hydraulic diameter of the primary austenite as the main parameter describing the tensile strength. The hydraulic diameter can be described as the size of the inter-dendritic regions in the structure. Hence it decides the size of the graphite flakes by restricting their growth. It has a close coupling to the amount of primary austenite but is also affected by cooling rate. The relation to UTS reminds of the Catalina equation by having a one over square root appearance, see Eq. 2.

$$\sigma = \frac{k}{\sqrt{D_{hyd}}} \quad (2)$$

This paper presents an experimental correlation between microstructure and tensile strength for a low alloyed grey iron including the influence of solidification time, cooling rate, pearlite hardness and graphite size and shape. These data provides an excellent basis for a more theoretical model of the mechanical properties of grey iron.

Experimental

The experimental material consists of two six-cylinder engine blocks, see Fig. 2. They were gravity cast in horizontally parted green sand moulds at the KFIL foundry in Hospet, India. Pouring temperature was around 1400 °C and shake-out time was 2,5 hours.

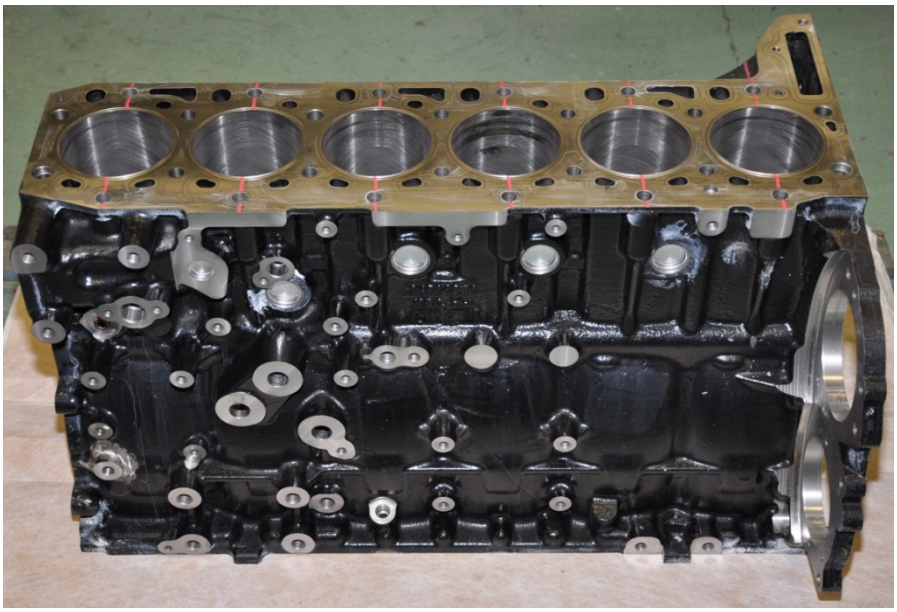

Figure 2. The six-cylinder engine block serving as test material.

The composition of the grey iron is given in Table 1.

Table 1. Chemical composition of the two cylinder blocks in weight-%.

	C	Si	Mn	P	S	Cr	Mo	Cu	Sn	Ti	CE
No. 1	3,24	1,95	0,71	0,04	0,05	0,20	0,01	0,67	0,065	0,026	3,75
No. 2	3,24	1,93	0,69	0,03	0,05	0,23	0,01	0,75	0,074	0,022	3,74

Four cylindrical tensile test bars were extracted from the middle wall (between cylinder 3 and 4) of each block, see Fig. 3. Test bar geometry is given in Fig. 4. Tensile testing was performed on a Zwick Z250 tensile testing machine with a speed of 2 mm/min.

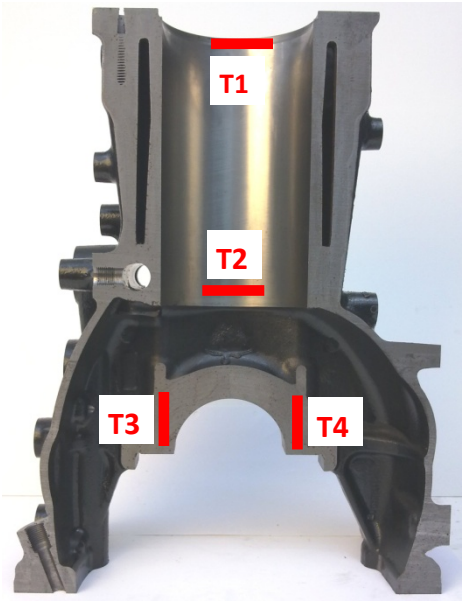

Figure 3. Position of the tensile test bars.

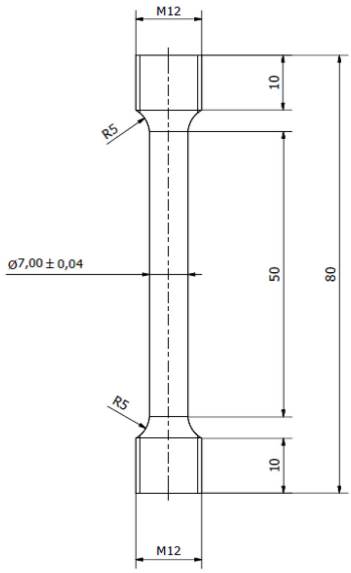

Figure 4. Tensile test bar geometry.

Positions T3 and T4 are equivalent from a geometrical point of view.

After tensile testing, the fracture surfaces were analyzed in a scanning electron microscope (SEM). Hardness was measured with a Wolpert Dia Testor 3a machine using a 5 mm hard metal ball and 750 kg of load. Microstructure was analyzed in a light optical microscope (LOM). For determination of matrix structure the samples were etched in a 3 % Nital solution.
Casting simulation was made with Magmasoft v4.4, standard module. The reason for choosing the standard module is that the more advanced Magmairon module introduces a number of unknown and difficult-to-control parameters regarding nucleation and growth.

Results

Tensile testing. The tensile testing results are given in Table 2. Both blocks show the same trend with position T1 being the strongest and position T2 the weakest.

Table 2. Tensile testing results (in MPa).

	Block No. 1				Block No. 2			
Position	T1	T2	T3	T4	T1	T2	T3	T4
UTS	218	173	187	199	219	165	180	186

Fractography. Fig. 5 shows the fracture surfaces of test bars T1 and T2 from block No. 1. It is quite clear that the fracture surface of test bar T1, which is 45 MPa stronger, contains much finer graphite than does test bar T2.

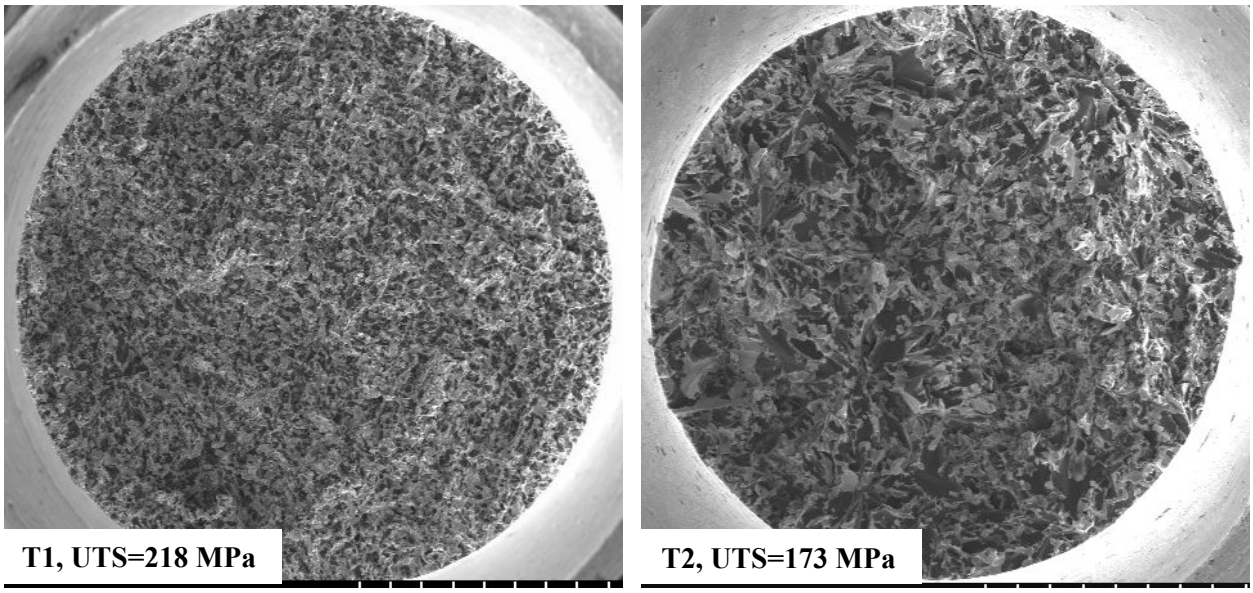

Figure 5. Fracture surfaces of test bars T1 (left) and T2 (right) from block No. 1. SEM images.

Test bars T3 and T4, which show intermediate strength, also show an intermediate fracture surface appearance with a mix of fine and coarse graphite, see Fig. 6.

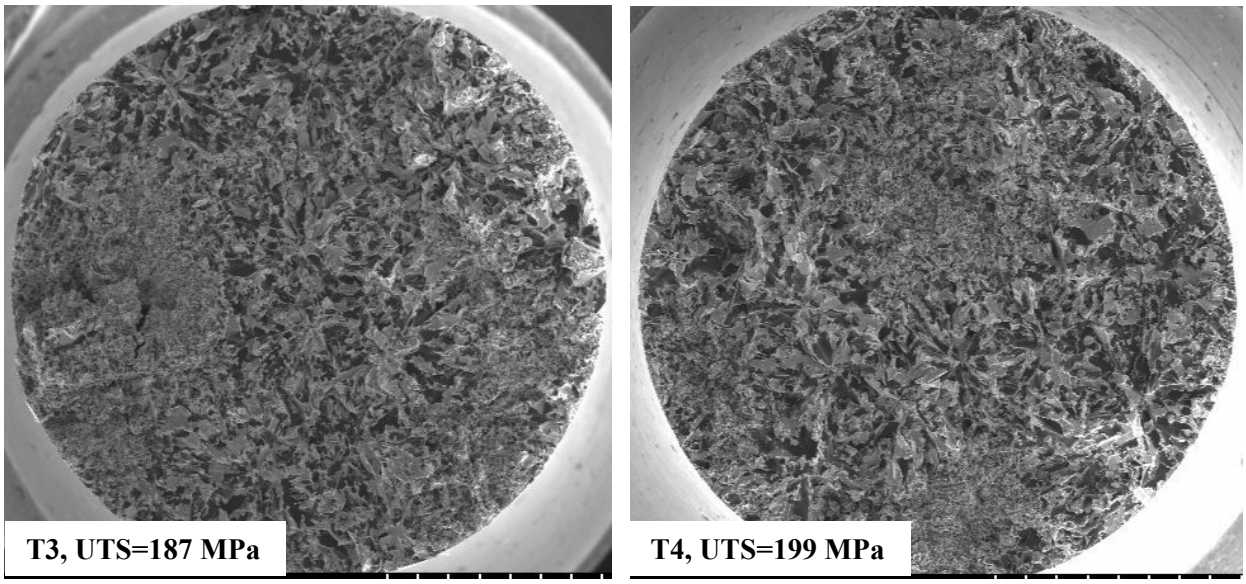

Figure 6. Fracture surfaces of test bars T3 (left) and T4 (right) from block No. 1. SEM images.

Hardness. The hardness shows a different behavior than does the tensile strength; test positions T3 and T4, which showed an intermediate strength, now shows the highest hardness values, see Table 3. Positions T1 and T2, which were furthest apart regarding UTS, are now more or less equal. This is also shown in Fig. 7.

Table 3. Hardness testing results (HBW 5/750).

	Block No. 1				Block No. 2			
Position	T1	T2	T3	T4	T1	T2	T3	T4
Hardness	178	173	190	191	178	174	191	190

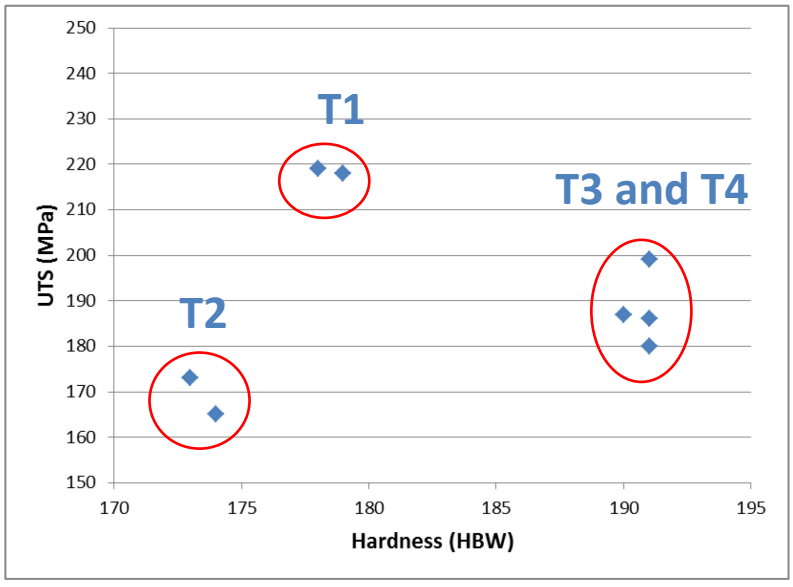

Figure 7. Relation between UTS and hardness for the different positions.

Microstructure. The graphite in the block is a mix of type A ('normal' flake graphite) and type E (inter-dendritic flake graphite). Fig. 8 shows polished sections through test bars T1-T3 in low magnification. The graphite structures correspond well with the appearances of the fracture surfaces.

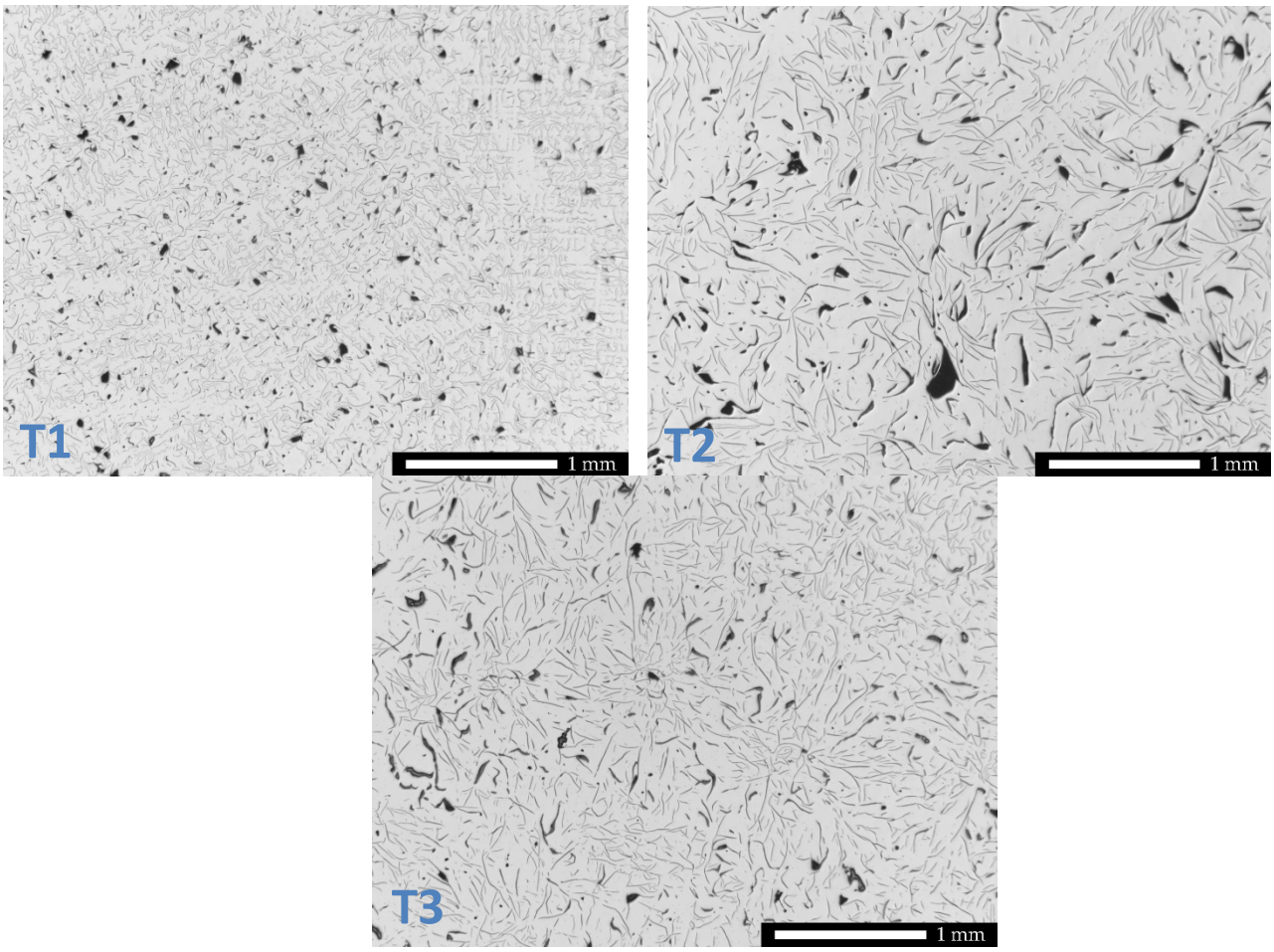

Figure 8. Un-etched polished sections showing the graphite structure at positions T1-T3.

The matrix is pearlitic with traces of free ferrite in the center of primary dendrite arms, see Fig. 9. A low level of carbides (Fe_3C) exists as well. The levels of free ferrite and cementite have not been quantified but represents < 1 % each.

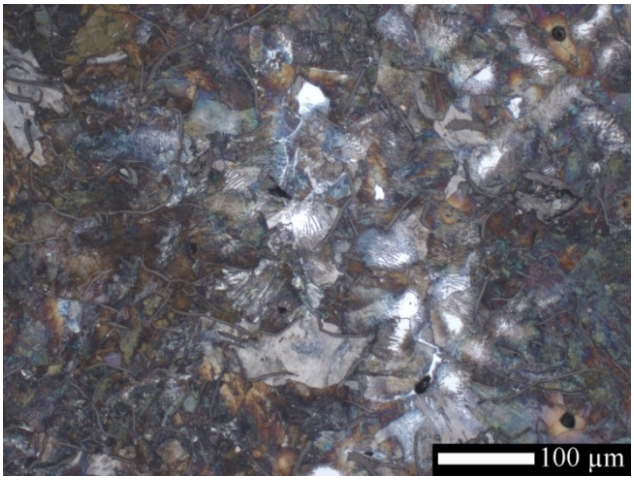

Figure 9. Etched polished section showing a pearlitic matrix structure with some free ferrite and cementite.

Casting simulation. Figure 10 shows solidification and cooling at the four test positions by means of virtual thermo-couples. Interesting to note is that position T1 has the shortest solidification time but then slows down in cooling rate and reaches the pearlite transformation later than positions T3 and T4. Position T2 has both the longest total solidification time *and* the longest pearlite transformation time.

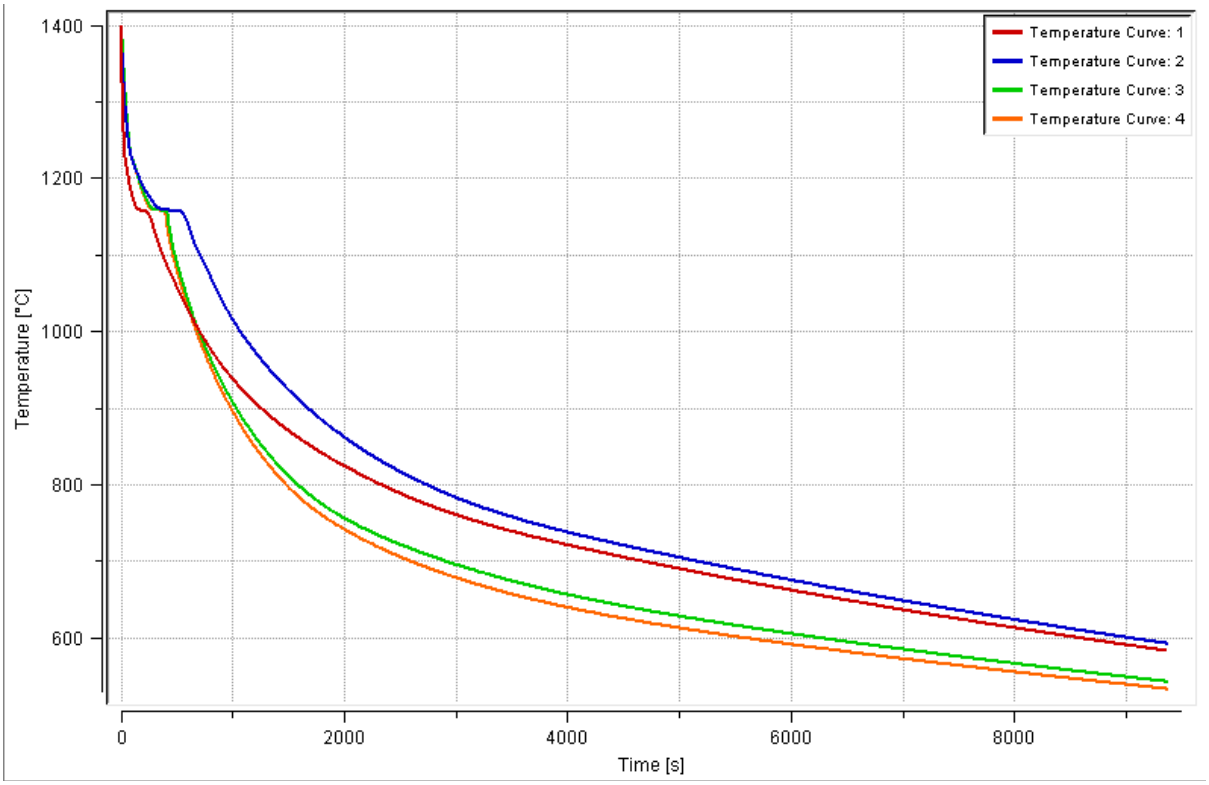

Figure 10. Simulated cooling curves.

The simulation parameters which have been analyzed are total solidification time (s) and pearlite transformation rate expressed as cooling rate (°C/min) at 720 °C, see Table 4.

Table 4. Summary of solidification results.

	T1	T2	T3	T4
Total solidification time (s)	218	510	348	322
Cooling rate at 720 °C (°C/min)	1,82	1,71	2,83	3,12

Correlation between solidification time/cooling rate and tensile strength/hardness.
In Fig. 11 the measured tensile strength (MPa) is plotted versus simulated solidification time expressed as 1/solidification time*1000(s^{-1}*1000). As can be seen there is a clear linear relationship. In Fig. 12 the measured hardness (HBW) is plotted versus simulated cooling rate at 720 °C (°C/min), the latter taken as a measure of the pearlite transformation rate. Also in this case there is a clear linear relationship.

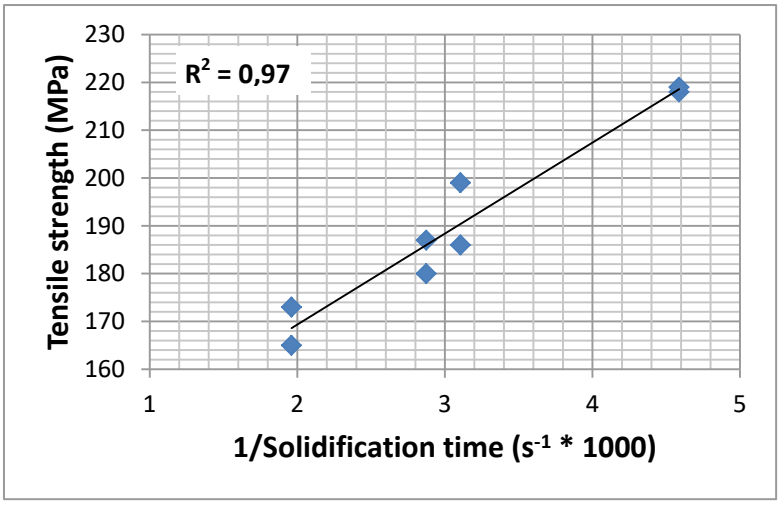

Figure 11. Measured tensile strength (MPa) vs. simulated 1/solidification time (s^{-1}*1000).

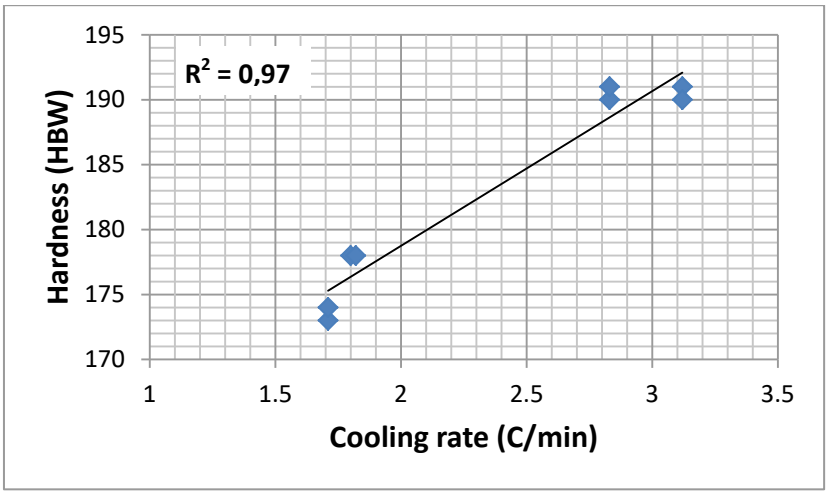

Figure 12. Measured hardness (HBW) vs. simulated cooling rate at 720 °C (°C/min).

Discussion and Conclusions

In traditional research the test geometries used (plates and/or staircases) give a coupling between solidification time and cooling rate which make the two parameters hard to separate. Furthermore, fractography on grey cast iron test bars are normally not fruitful. By a coincidence, these two things were different in this case. Therefore it is possible to draw two important conclusions from the results above:

1. Tensile strength is mainly dependent on solidification time and the resulting graphite fineness.
2. Hardness is mainly dependent on cooling rate during pearlite transformation and the resulting pearlite fineness.

No quantitative relations between microstructure and solidification/cooling parameters have been made in this report. However, if one assumes that UTS is proportional to $(L_{max})^{-1/2}$, then Fig. 11 suggests that L_{max} is proportional to t_s^2. This a rather strong relation which might be true for relatively short solidification times as in the present investigation. However, for longer solidification times (>500 s) L_{max} tends to converge to a constant value [6]. This is probably due to impingement of the graphite cells.

In order to find a similar relation for the pearlite lamellar spacing one first needs to assume a relation between hardness and tensile strength. Therefore, this becomes less meaningful.

References

[1] R. Schneidewind and R.G. McElwee, AFS Transactions, 58(1950), 312-332.
[2] Bates, C.E., “Alloy Element Effects on Gray Iron Properties: Part II,” AFS Transactions, 94 (1986), 889-912.
[3] Catalina A., Guo, X., Stefanescu, D.M., Chuzhoy, L., Pershing, M.A., “Prediction of Room Temperature Microstructure and Mechanical Properties in Gray Iron Castings,” AFS Transactions, 108 (2000), 247-257.
[4] Mampaey, F.; “Prediction of Gray Iron Tensile Strength by the Separation of Variables” Copyright 2004 American Foundry Society.
[5] Fourlakidis, V. and Dioszegi, A.; “A generic model to predict the ultimate tensile strength in pearlitic lamellar graphite iron” Mat Sci Eng A – Struct 618 (2014) 161–167.
[6] Orea, N.; “Development of a Computer Model for Tensile Strength Prediction of Grey Cast Iron.” Master Thesis at Volvo Powertrain Corporation (2016). To be published.